

## Effect of Mechanical Boundary Conditions on Phase Diagrams of Epitaxial Ferroelectric Thin Films

N. A. Pertsev,<sup>1</sup> A. G. Zembilgotov,<sup>2</sup> and A. K. Tagantsev<sup>3</sup>

<sup>1</sup>*A. F. Ioffe Physico-Technical Institute, Russian Academy of Sciences, 194021 St. Petersburg, Russia*

<sup>2</sup>*State Technical University of St. Petersburg, 195251 St. Petersburg, Russia*

<sup>3</sup>*Laboratoire de Céramique, Ecole Polytechnique Fédérale de Lausanne, Lausanne CH 1015, Switzerland*

(Received 1 May 1997; revised manuscript received 14 January 1998)

A phenomenological thermodynamic theory of ferroelectric thin films epitaxially grown on cubic substrates is developed using a new form of the thermodynamic potential, which corresponds to the actual mechanical boundary conditions of the problem. For single-domain BaTiO<sub>3</sub> and PbTiO<sub>3</sub> films, the “misfit-temperature” phase diagrams are constructed. It is found that the 2D clamping of the films, apart from a shift of the temperature of the ferroelectric transition, results in a change of its order. A change of the sequence of the phases and the appearance of phases forbidden in the bulk crystals are predicted. [S0031-9007(98)05421-0]

PACS numbers: 77.55.+f, 77.22.Ch, 77.80.Dj

During the past decade, ferroelectric thin films attracted considerable attention of physicists. On one hand, their ferroelectric, dielectric, and piezoelectric properties were found to be promising for microelectronic and micromechanical applications [1]. On the other hand, the physical properties of ferroelectric thin films were found to be substantially different from those of bulk ferroelectrics. Both experimental [2,3] and theoretical [4–8] studies identified several phenomena which occur in thin films due to size effects or the pseudo-2D nature of the object. However, up to now, no adequate thermodynamic theory was developed despite several attempts made in this direction [9–12]. The point is that all of these studies do not allow for the actual mechanical boundary conditions existing in a thin film epitaxially grown on a substrate.

In this Letter, a new form of the thermodynamic potential is derived and used to develop phase diagrams for epitaxial single-domain thin films of two classical perovskite ferroelectrics—BaTiO<sub>3</sub> (BT) and PbTiO<sub>3</sub> (PT). The dielectric properties of the films are analyzed and related to those of a system with two coupled instabilities—ferroelectric and structural [13].

We consider here only films with thicknesses  $h$  much larger than the ferroelectric correlation length, i.e., practically films with  $h > 50$  nm. In this case, the “microscopic” size effects similar to those considered in Refs. [4,8] may be neglected. We also do not discuss some macroscopic effects additional to the mechanical clamping of the film. However, our theory provides the basis for the analysis of these effects. For example, it is straightforward to show that the depolarizing-field-induced shift of the transition temperature [7] can be easily incorporated into it.

First, let us find the thermodynamic potential which minima correspond to the equilibrium thermodynamic states of a thin film epitaxially grown on a substrate. Since there are no tractions acting on the free surface of the film, the

stresses  $\sigma_3$ ,  $\sigma_4$ , and  $\sigma_5$  must be zero on this surface. (We use the Voigt matrix notation and the rectangular Cartesian frame of reference with the  $x_3$  axis perpendicular to the film/substrate interface.) On the other hand, the lattice matching between the film and a thick substrate implies that the in-plane strains  $u_1$ ,  $u_2$ , and  $u_6$  of the film at the film/substrate interface are totally controlled by the substrate, which is assumed to be sufficiently thick. In the considered case of a single-crystalline single-domain film, internal elastic fields are homogeneous so that the above conditions hold throughout the film volume. For these “mixed” mechanical conditions, clearly, the minima of the standard elastic Gibbs function  $G$  [10] (with polarization and stress used as independent variables) do not correspond to the equilibrium thermodynamic states (they are associated with the equilibrium thermodynamic states at fixed stresses). It is easy to show that, for the discussed 2D-clamping case, the sought thermodynamic potential is given by the following Legendre transformation of  $G$

$$\tilde{G} = G + u_1\sigma_1 + u_2\sigma_2 + u_6\sigma_6. \quad (1)$$

This is a general expression for the thermodynamic potential of a thin ferroelectric film on a thick substrate.

In this paper, we consider the case of a (001) ferroelectric thin film epitaxially grown in a cubic paraelectric phase on a cubic (001) substrate. In this case, evidently,  $u_1 = u_2$  and  $u_6 = 0$ . If the film/substrate interface is commensurate [14], then  $u_1 = u_2 \equiv u_m$ , where the misfit strain  $u_m = (b - a_0)/b$  can be calculated from the substrate lattice parameter  $b$  and the equivalent cubic cell constant  $a_0$  of the free standing film. If some interface relaxation takes place, the real substrate lattice parameter  $b$  should be replaced in this equation by the effective substrate lattice parameter  $b^*$  [15]. One can find the final form of  $\tilde{G}(\vec{P}, u_m, T)$  by using Eq. (1) and the well-known expression for the elastic Gibbs function of a “cubic”

ferroelectric [16]:

$$\begin{aligned}
G = & a_1(P_1^2 + P_2^2 + P_3^2) + a_{11}(P_1^4 + P_2^4 + P_3^4) + a_{12}(P_1^2P_2^2 + P_1^2P_3^2 + P_2^2P_3^2) + a_{111}(P_1^6 + P_2^6 + P_3^6) \\
& + a_{112}[P_1^4(P_2^2 + P_3^2) + P_3^4(P_1^2 + P_2^2) + P_2^4(P_1^2 + P_3^2)] + a_{123}P_1^2P_2^2P_3^2 - \frac{1}{2}s_{11}(\sigma_1^2 + \sigma_2^2 + \sigma_3^2) \\
& - s_{12}(\sigma_1\sigma_2 + \sigma_1\sigma_3 + \sigma_3\sigma_2) - \frac{1}{2}s_{44}(\sigma_4^2 + \sigma_5^2 + \sigma_6^2) - Q_{11}(\sigma_1P_1^2 + \sigma_2P_2^2 + \sigma_3P_3^2) \\
& - Q_{12}[\sigma_1(P_2^2 + P_3^2) + \sigma_3(P_1^2 + P_2^2) + \sigma_2(P_1^2 + P_3^2)] - Q_{44}(P_2P_3\sigma_4 + P_1P_3\sigma_5 + P_2P_1\sigma_6), \quad (2)
\end{aligned}$$

where all of the stress components should be eliminated with the aid of the aforementioned mechanical conditions in the film:  $\partial G/\partial\sigma_1 = \partial G/\partial\sigma_2 = -u_m$ ,  $\partial G/\partial\sigma_6 = 0$ , and  $\sigma_3 = \sigma_4 = \sigma_5 = 0$ .

The knowledge of the potential  $\tilde{G}(\vec{P}, u_m, T)$  as a function of temperature  $T$ , polarization  $P_i$ , and misfit strain  $u_m$  enables the complete thermodynamic description of the films in question, including the  $(u_m, T)$ -phase diagram for the single-domain state. We have calculated this phase diagram for BT and PT films using the parameters [17] of the elastic Gibbs function, which were taken from Refs. [16,18–21].

The 2D clamping, evidently, lowers the symmetry of the paraelectric phase from cubic to tetragonal. As a result, five low-temperature phases become possible in the film instead of three in the bulk material. For these five phases,

we introduce the following notation: (i) the  $c$  phase, where  $P_3 \neq 0$  and  $P_1 = P_2 = 0$ ; (ii) the  $a$  phase, where  $P_1 \neq 0$  and  $P_3 = P_2 = 0$ ; (iii) the  $ac$  phase, where  $P_1 \neq 0$ ,  $P_3 \neq 0$ , and  $P_2 = 0$ ; (iv) the  $aa$  phase, where  $P_1 = P_2 \neq 0$  and  $P_3 = 0$ ; and (v) the  $r$  phase, where  $P_1 = P_2 \neq 0$  and  $P_3 \neq 0$ . To determine equilibrium thermodynamic states of the BT and PT films, we calculated all of the minima of  $\tilde{G}(\vec{P}, u_m, T)$  with respect to the components of the polarization and then selected the phase which corresponds to minimum minimorum. We found that, in PT, the  $a$  and  $ac$  phases are always unstable, whereas, in BT, only the  $a$  phase is unstable at all investigated temperatures and values of the misfit strain. The phase diagrams showing the stability ranges of the remaining equilibrium states are presented in Fig. 1.

In order to explain these diagrams, we discuss the thermodynamic potential  $\tilde{G}(\vec{P}, u_m, T)$ , which can be written as

$$\begin{aligned}
\tilde{G} = & a_1^*(P_1^2 + P_2^2) + a_3^*P_3^2 + a_{11}^*(P_1^4 + P_2^4) + a_{33}^*P_3^4 + a_{13}^*(P_1^2P_3^2 + P_2^2P_3^2) + a_{12}^*P_1^2P_2^2 + a_{111}(P_1^6 + P_2^6 + P_3^6) \\
& + a_{112}[P_1^4(P_2^2 + P_3^2) + P_3^4(P_1^2 + P_2^2) + P_2^4(P_1^2 + P_3^2)] + a_{123}P_1^2P_2^2P_3^2 + \frac{u_m^2}{s_{11} + s_{12}}; \\
& a_1^* = a_1 - u_m \frac{Q_{11} + Q_{12}}{s_{11} + s_{12}}, \quad a_3^* = a_1 - u_m \frac{2Q_{12}}{s_{11} + s_{12}}, \quad (3) \\
& a_{11}^* = a_{11} + \frac{1}{2} \frac{1}{s_{11}^2 - s_{12}^2} [(Q_{11}^2 + Q_{12}^2)s_{11} - 2Q_{11}Q_{12}s_{12}], \quad a_{33}^* = a_{11} + \frac{Q_{12}^2}{s_{11} + s_{12}}, \\
& a_{12}^* = a_{12} - \frac{1}{s_{11}^2 - s_{12}^2} [(Q_{11}^2 + Q_{12}^2)s_{12} - 2Q_{11}Q_{12}s_{11}] + \frac{Q_{44}^2}{2s_{44}}, \quad a_{13}^* = a_{12} + \frac{Q_{12}(Q_{11} + Q_{12})}{s_{11} + s_{12}}.
\end{aligned}$$

It can be seen that the mechanical 2D clamping renormalizes the second-order and the fourth-order polarization terms. The values of the renormalized fourth-order coefficients for BT and PT are shown in Table I, where the nonrenormalized coefficients ( $a_{11}$  and  $a_{12}$ ) are given in parentheses for comparison.

From the analysis of Eqs. (3), the following features of the phase transitions in BT and PT films can be singled out.

(i) The phase transition from the paraelectric state to single-domain ferroelectric states is of the second order in BT and PT films (instead of the first order in bulk crystals [21]). This is due to the positive sign of the coefficients  $a_{11}^*$ ,  $a_{12}^*$ , and  $a_{33}^*$  (see Table I) [22].

(ii) This transition takes place at temperature  $T_c = \max[T_1, T_3]$ ,  $T_3$  and  $T_1$  being the temperatures at which the paraelectric phase loses its stability with respect to the appearance of  $P_3$  and  $P_1 = P_2$ . Setting  $a_1^* = 0$  and  $a_3^* = 0$ , with the aid of Eqs. (3), we find

$$\begin{aligned}
T_3 = & T_0 + 2C\varepsilon_0 \frac{2Q_{12}}{s_{11} + s_{12}} u_m, \\
T_1 = & T_0 + 2C\varepsilon_0 \frac{Q_{11} + Q_{12}}{s_{11} + s_{12}} u_m, \quad (4)
\end{aligned}$$

where  $C$  and  $\varepsilon_0$  are the Curie-Weiss constant and the dielectric susceptibility of the vacuum  $[(2C\varepsilon_0)^{-1} = \partial a_1/\partial T]$ . Because in PT and BT  $Q_{11} + Q_{12}$  is positive whereas  $Q_{12}$  is negative,  $T_c$  is always higher than the Curie-Weiss temperature  $T_0$  of the bulk material. This explains a ‘‘seagull’’ shape of the transition line  $T_c(u_m)$ . The results (i) and (ii) differ qualitatively from that of Ref. [10] where, for the same system, a monotonical misfit dependence of the first-order ferroelectric phase transition temperature was predicted.

(iii) The phase diagrams of BT and PT are very different with respect to the transitions between various

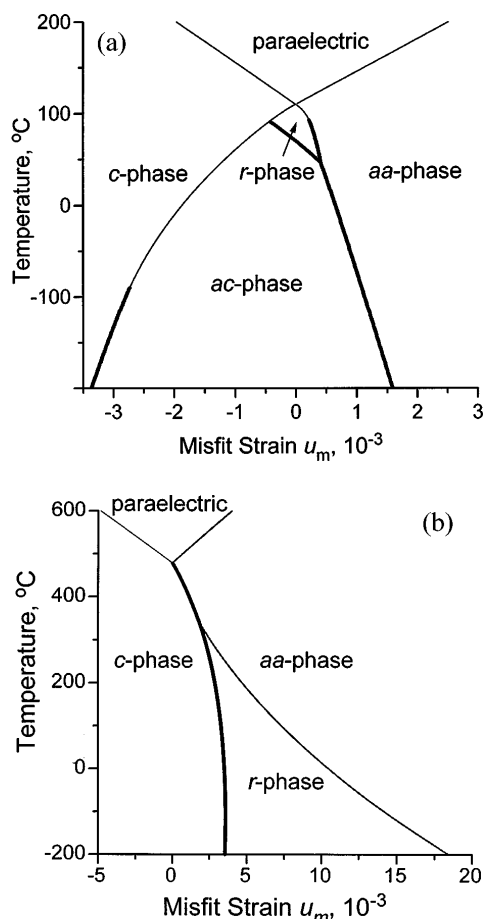


FIG. 1. Phase diagrams of (001) single-domain BaTiO<sub>3</sub> (a) and PbTiO<sub>3</sub> (b) thin films epitaxially grown on different cubic substrates providing various misfit strains  $u_m$  in the heterostructures. The second- and first-order phase transitions are shown by thin and thick lines, respectively. The quadruple and triple points at  $u_m = 0$  correspond to the Curie-Weiss temperatures of these materials in the bulk form.

low-temperature ferroelectric phases (see Fig. 1). In the case of BT, at the point ( $T = T_0, u_m = 0$ ) four phases meet (quadruple point), and in the vicinity of this point the diagram looks like a simple superposition of the two independent transition lines corresponding to the appearance of  $P_1 = P_2$  and  $P_3$ . In contrast, for PT, the point ( $T = T_0, u_m = 0$ ) is a triple point. This difference can be explained by analyzing the interaction between the polarizations  $P_1 = P_2$  and  $P_3$ , which play, in our problem, the role of two order parameters linked by the nonlinear coupling term  $a_{13}^*(P_1^2 + P_2^2)P_3^2$ . Following Ref. [13], we evaluate the strength of this interaction by the dimensionless parameter  $\varphi = a_{13}^*/\sqrt{(2a_{11}^* + a_{12}^*)a_{33}^*}$ . From the numerical values given in the table, it fol-

lows that, in BT,  $\varphi$  is very small in the vicinity of the quadruple point. This indicates a minor role of the discussed interaction so that the  $P_1$ - and  $P_3$ -related phase transitions appear to be virtually independent at least near this point. In PT,  $\varphi$  is positive and larger than unity. Accordingly, there is a substantial interaction between two competing order parameters, i.e., in the presence of one of them, the spontaneous appearance of the other is energetically less favorable or even impossible. This strong interaction leads to the elimination of the mixed  $r$  phase in PT in the vicinity of the ( $T = T_0, u_m = 0$ ) point, which becomes a triple one here instead of a quadruple point in BT.

(iv) In PT films at low temperatures, the 2D clamping stabilizes the  $aa$  phase and the  $r$  phase with two and three nonzero components of the polarization, which do not exist in a free bulk crystal [16]. The  $aa$  phase is orthorhombic, whereas the  $r$  phase is a monoclinic.

(v) An interesting feature of the phase diagram obtained for BT is that, at zero misfit strain, the predicted temperature-driven phase transformation in the film is qualitatively different from that occurring in the bulk crystal. This fact can be explained as follows. From inspection of Eqs. (3), it can be seen that the effect of 2D clamping is twofold. The mismatch between the substrate lattice parameter  $b$  and the lattice constant  $a_0$  of the paraelectric phase is responsible for the splitting of the instability temperature and its shift [see the dependence of  $a_1^*$  and  $a_3^*$  on  $u_m$  in Eqs. (3)]. On the other hand, the 2D clamping suppresses the in-plane film strains, which results in a renormalization of the  $P^4$  terms. This renormalization changes the order of the paraelectric to ferroelectric phase transition in BT films and influences the type of the low-temperature phase. Since, according to Eqs. (3), the renormalization is independent of the misfit strain  $u_m$ , the phase transformation in a thin film may be altered even at  $u_m = 0$ .

Consider now the dielectric properties of epitaxial films. In a conventional setup, the electric field is orthogonal to the film surfaces so that it does not interact directly with the in-plane components  $P_1 = P_2$  of polarization. Thus, in this situation,  $P_1$  should be considered as a “purely structural” order parameter. At the same time, the instability temperatures, which correspond to the appearance of the in-plane  $P_1 = P_2$  and out-of-plane  $P_3$  polarizations on cooling, are different [c.f. Eqs. (4)]. All in all, we may conclude that, with respect to the observed dielectric response  $\epsilon_{33}$ , the behavior of thin films is equivalent to that of a system with two coupled instabilities (ferroelectric and structural). The analysis of this system [13]

TABLE I. Parameters of  $P^4$  terms of the renormalized thermodynamic potential of BaTiO<sub>3</sub> and PbTiO<sub>3</sub> thin films epitaxially grown on a cubic substrate.

Units for $a$ 's $10^8 \text{ m}^5/\text{FC}^2$	$a_{11}^*$	$a_{33}^*$	$a_{12}^*$	$a_{13}^*$	$\varphi = a_{13}^*/\sqrt{(2a_{11}^* + a_{12}^*)a_{33}^*}$
BaTiO <sub>3</sub> ( $T = 110^\circ\text{C}$ )	4.9 (-2.4)	0.9 (-2.4)	0.15 (4.9)	-0.24 (4.9)	-0.08
PbTiO <sub>3</sub>	4.2 (-0.73)	0.5 (-0.73)	7.3 (7.5)	4.5 (7.5)	1.6

showed that, depending on the parameters of the thermodynamic potential, it can display a rich spectrum of dielectric properties ranging from normal ferroelectric to antiferroelectric behavior [13,23] or trigger phase transitions [24]. Thus, epitaxial thin films may demonstrate the aforementioned variety of dielectric properties. For BT and PT, the following anomalies of  $\epsilon_{33}$  are expected at the transition lines shown in Fig. 1: (i) At the paraelectric/*c*-phase, the *aa*-phase/*ac*-phase, and the *aa*-phase/*r*-phase transition lines,  $\epsilon_{33}$  should exhibit a Curie-Weiss-type anomaly in both the temperature and misfit strain dependences [see the expression for  $a_3^*$  in Eqs. (3)]. Depending on the external conditions, the anomaly can have the features corresponding to the second or first order ferroelectric phase transitions. Figure 2 shows this anomaly for BT in the case of the first order phase transition. (ii) The paraelectric/*aa*-phase transition as a “structural” one results in a change of slope of the  $\epsilon_{33}(T)$  and  $\epsilon_{33}(u_m)$  dependences. (iii) the *c*-phase/*ac*-phase, *c*-phase/*r*-phase, and *ac*-phase/*r*-phase transitions should be considered as structural transitions between two polar phases. Even when being of the second order such transition should give a jump of  $\epsilon_{33}$  on crossing the transition line [13]. (For BT, in the case illustrated by Fig. 2, this jump equals 8.)

In summary, a new form of the thermodynamic potential consistent with the mechanical conditions in epitaxial thin films was developed. Using this potential, the “temperature-misfit strain” phase diagrams for epitaxial single-domain BaTiO<sub>3</sub> and PbTiO<sub>3</sub> ferroelectric thin films were calculated and the dielectric response of these films was analyzed. A drastic difference between the thermodynamic properties of thin films and bulk crystals is predicted.

When this paper was finished, we became aware of the article [25] where the phase transitions in a BaTiO<sub>3</sub> epitaxial thin film were theoretically studied. In some points, the results of that paper are consistent with ours, but there is a difference in others.

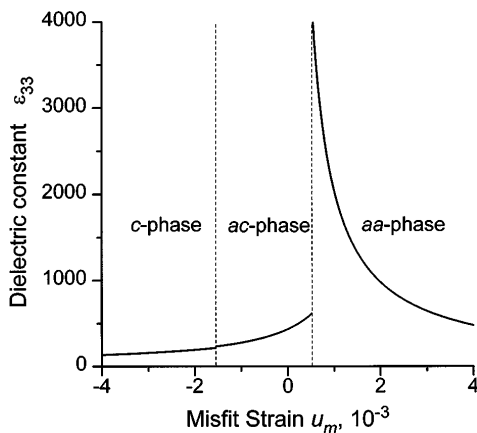


FIG. 2. Calculated dependence of the electric permittivity  $\epsilon_{33}$  of epitaxial (001) single-domain BaTiO<sub>3</sub> films on the misfit strain  $u_m$  at room temperature.

A. K. T. acknowledges Swiss National Science Foundation for financial support.

- [1] J. F. Scott, *Ferroelectrics* **183**, 51 (1996).
- [2] P. W. M. Blom, R. M. Wolf, J. F. M. Cillesen, and M. P. C. M. Krijn, *Phys. Rev. Lett.* **73**, 2107 (1994).
- [3] A. L. Kholkin, E. Colla, A. K. Tagantsev, D. V. Taylor, and N. Setter, *Appl. Phys. Lett.* **68**, 2577 (1996).
- [4] Y. G. Wang, W. L. Zhong, and P. L. Zhang, *Phys. Rev. B* **51**, 5311 (1995).
- [5] N. A. Pertsev, G. Arlt, and A. G. Zembilgotov, *Phys. Rev. Lett.* **76**, 1364 (1996).
- [6] A. K. Tagantsev, Cz. Pawlaczyk, K. Brooks, and N. Setter, *Integr. Ferroelectr.* **4**, 1 (1994).
- [7] D. R. Tilley and B. Zeks, *Ferroelectrics* **134**, 313 (1992).
- [8] K. Binder, *Ferroelectrics* **35**, 99 (1981).
- [9] Y. Yano, K. Iijima, Y. Daitoh, T. Terashima, Y. Bando, Y. Watanabe, H. Kasatani, and H. Terauchi, *J. Appl. Phys.* **76**, 7833 (1994).
- [10] G. A. Rossetti, Jr., L. E. Cross, and K. Kushida, *Appl. Phys. Lett.* **59**, 2524 (1991).
- [11] T. Yamamoto and H. Matsuoka, *Jpn. J. Appl. Phys.* **33**, 5317 (1994).
- [12] N. A. Pertsev, G. Arlt, and A. G. Zembilgotov, *Microelectron. Eng.* **29**, 135 (1995).
- [13] E. V. Balashova and A. K. Tagantsev, *Phys. Rev. B* **48**, 9979 (1993).
- [14] S. Little and A. Zangwill, *Phys. Rev. B* **49**, 16 659 (1994).
- [15] J. S. Speck and W. Pompe, *J. Appl. Phys.* **76**, 466 (1994).
- [16] M. J. Haun, E. Furman, S. J. Jang, H. A. McKinstry, and L. E. Cross, *J. Appl. Phys.* **62**, 3331 (1987).
- [17] The list of the parameters of  $G$  (in SI units, the temperature  $T$  in °C) used in the calculations. For BaTiO<sub>3</sub>:  $a_1 = 3.3(T - 110) \times 10^5$ ;  $a_{11} = 3.6(T - 175) \times 10^6$ ;  $a_{12} = 4.9 \times 10^8$ ;  $a_{111} = 6.6 \times 10^9$ ;  $a_{112} = 2.9 \times 10^9$ ;  $a_{123} = 7.6(T - 120) \times 10^7 + 4.4 \times 10^{10}$ ;  $Q_{11} = 0.11$ ,  $Q_{12} = -0.043$ ;  $Q_{44} = 0.059$ ;  $s_{11} = 8.3 \times 10^{-12}$ ;  $s_{12} = -2.7 \times 10^{-12}$ ,  $s_{44} = 9.24 \times 10^{-12}$ . For PbTiO<sub>3</sub>:  $a_1 = 3.8(T - 479) \times 10^5$ ;  $a_{11} = -7.3 \times 10^7$ ;  $a_{12} = 7.5 \times 10^8$ ;  $a_{111} = 2.6 \times 10^8$ ;  $a_{112} = 6.1 \times 10^8$ ;  $a_{123} = -3.7 \times 10^9$ ;  $Q_{11} = 0.089$ ,  $Q_{12} = -0.026$ ;  $Q_{44} = 0.0675$ ;  $s_{11} = 8.0 \times 10^{-12}$ ;  $s_{12} = -2.5 \times 10^{-12}$ ,  $s_{44} = 9.0 \times 10^{-12}$ .
- [18] W. R. Buessem, L. E. Cross, and A. K. Goswami, *J. Am. Ceram. Soc.* **49**, 33 (1966).
- [19] M. Pikalev and V. I. Aleshin, *Fiz. Tverd. Tela* **31**, No. 12, 95 (1989) [*Sov. Phys. Solid State* **31**, 2079 (1989)].
- [20] M. J. Haun, Z. Q. Zhuang, E. Furman, S. J. Jang, and L. E. Cross, *Ferroelectrics* **99**, 45 (1989).
- [21] F. Jona and G. Shirane, *Ferroelectric Crystals* (Macmillan, New York, 1962).
- [22] For BaTiO<sub>3</sub>, these coefficients are slightly temperature dependent but they do not change the sign at the transition lines in question.
- [23] V. E. Yurkevich, B. N. Rolov, and H. E. Stanly, *Ferroelectrics* **16**, 61 (1977); Yu. M. Gufan and E. S. Larin, *Fiz. Tverd. Tela* **22**, 463 (1980) [*Sov. Phys. Solid State* **22**, 270 (1980)].
- [24] J. Holakovsky, *Phys. Status Solidi b* **56**, 615 (1973).
- [25] S. B. Desu, V. P. Dudkevich, P. V. Dudkevich, I. N. Zakharchenko, and G. L. Kushlyan, *Mater. Res. Soc. Symp. Proc.* **401**, 195 (1996).